Journal of Inorganic and Organometallic Polymers and Materials (2022) 32:1206–1212
https://doi.org/10.1007/s10904-021-02159-y

The Dielectric Properties and Thermal Conductivities of Epoxy Composites Reinforced by Titanium Dioxide

Yuan Jia[1] · Juxiang Yang[1] · Weijie Dong[1] · Beibei Li[1] · Zhen Liu[1]

Received: 7 October 2021 / Accepted: 12 November 2021 / Published online: 20 November 2021

Abstract

To improve the dielectric properties and thermal conductivities of epoxy resins (EP), titanium dioxide superfine powders with microspheres structure (S-TiO_2) were prepared via a hydrothermal process based on the sodium dodecyl benzene sulfonate and hydroxyl silicate. The different content of S-TiO_2 was then employed as modifiers to add into EP resin to prepare the S-TiO_2/EP composites. The structure and morphology of the prepared S-TiO_2 was observed by X-ray diffraction (XRD) and scanning electron microscopy (SEM), and influences of different addition of S-TiO_2 on the thermal conductivity of S-TiO_2/EP composites are researched, while their dielectric constant and dielectric loss are also studied. The results suggested that the reasonable content of S-TiO_2 can endow the S-TiO_2/EP composites with higher dielectric constant without excessive increase their dielectric loss even under the high frequency. Furthermore, the thermal conductivity of S-TiO_2/EP are also be improved, which can be attributed to the good thermal conductivity of S-TiO_2 itself and the thermal conductivity path formed by S-TiO_2 inside the EP matrix.

Keywords Thermal conductivity · Dielectric constant · Dielectric loss · TiO_2 · Epoxy

1 Introduction

With the rapid development of electronic science and technology, various of new energy products emerge one after another, and the electronic devices tend to be miniaturized, integrated and flexible [1, 2]. In order to reduce the damage of material properties caused by a large amount of heat generated during the electrical operation, the excellent thermal conductivity of materials is increasingly required [3, 4]. As one of the universal thermosetting polymers, epoxy (EP) has been widely used as electronic components due to its high mechanical properties, low creep property and good oxidation resistance [5–7]. The thermal conductivity of pure EP is within the range of 0.17–0.23 W/mK, which can basically meet the requirements of common electronic components and materials [8, 9]. However, when used in the field of microelectronics and electrical appliances, their thermal conductivity still needs to be further optimized.

At present, a large number of literature reports have shown that appropriate modification methods can promote the industrial production of heat-conducting EP [10]. All the methods can be fall into two categories. The first is developing the intrinsic thermal conductivity EP, which is to introduce the elements and groups with good thermal conductivity into the main molecule or chain structure of the epoxy resin by forming the molecular bonds [11], or improve the order and high orientation of the structure of the EP [12]. Nevertheless, relying only on the construction of thermal connections in the EP structure cannot meet the needs of greater heat conduction [13, 14]. The second is to fill the fillers with excellent thermal conductivity such as boron nitride, aluminum nitride and alumina in to EP matrix [15–17], which is more simple and more flexible, hence this method has been applied more widely [18]. Although the addition of these fillers significantly improves the thermal conductivity of EP, it will also affect its dielectric properties in a certain extent [19]. Therefore, in order to minimize other additional damage caused by the fillers added into to EP, newer thermal conductivity fillers should be selected and prepared.

✉ Yuan Jia
jiayu_an_happy@126.com

[1] The Key Laboratory for Surface Engineering and Remanufacturing in Shaanxi Province, College of Chemical Engineering, Xi'an University, Xi'an 710065, Shaanxi, People's Republic of China

Metals and their oxides are often used as fillers for EP because of their excellent thermal conductivity [20]. Among them, titanium dioxide (TiO_2) is a kind of important inorganic functional material oxide, which exhibits excellent electric chemical and controllability, as while as the stronger photocatalysis [21, 22]. Numbers of research showed that by adding TiO_2 particles, the electrochemical properties of organic resin can be further improved [23, 24]. In addition, the excellent thermal stability of TiO_2 is benefit to the thermal conductivity of resins [25, 26]. From what has been discussed above, a new kind of TiO_2 particles with microspheres structure (S-TiO_2) were prepared via a hydrothermal process in this article, and the S-TiO_2 were then added into EP as modifiers to prepare a kind of novel S-TiO_2/EP composites. The thermal conductivity and dielectric properties of the S-TiO_2/EP composites were measured to research the effect of S-TiO_2 on the EP resins. This study is aiming to provide a new method for the development of new EP composites with the high thermal conductive, high dielectric constant and low dielectric loss, which can be used in microelectronic component fields.

2 Experimental Methods

2.1 Materials

The EP resin (the purity of > 95 wt%) was purchased from Nantong Xingchen Synthetic Material Co. Ltd. The isophorone diamine (analytical pure) was purchased from Shanghai McLean Biochemical Technology Co., Ltd. The n-butyl titanate (analytical pure) was purchased from Jingzhou fine chemical co., Ltd). The other solvents such as anhydrous ethanol and acetone were supplied by Tianjin Fuchen Chemical Reagents Factory without further purification.

2.2 Preparation of the S-TiO_2

The S-TiO_2 were obtained via the hydrothermal method. 12.5 mL n-butyl titanate and 1.5 mL water were added into a 50 mL hydrothermal kettle, the mixture was then reacted under 180 ℃ for 24 h. After naturally falling to room temperature, the mixture was centrifuged by anhydrous ethanol and deionized water for three times, respectively. The S-TiO_2 which are white powdery were finally obtained by dried at 60 ℃ for 12 h. The preparation process is shown in Fig. 1.

2.3 Preparation of the S-TiO_2/EP Composites

The S-TiO_2/EP composites with different content of S-TiO_2 were prepared via the casting method, which is shown in Fig. 2. The EP and isofrone diamine were stirred with the

Fig. 1 The preparation process of S-TiO_2

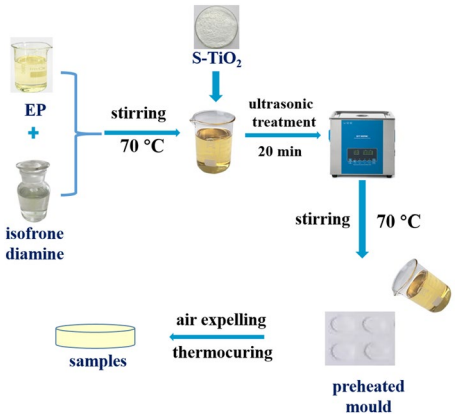

Fig. 2 The preparation process of S-TiO_2/EP

mass ratio of 7:1 in a glass beaker under 70 °C for 10 min, and the prepared S-TiO_2 (with the mass ratio of 0.0 wt%, 1.0 wt%, 2.0 wt%, 3.0 wt%, 4.0 wt%, 5.0 wt% and 6.0 wt%, respectively) in 20 mL acetone were added into the EP. These mixtures were ultrasonic dispersed under 70 °C for 20 min to ensure well-dispersed of S-TiO_2 in the EP matrix, thus the pre-polymer of S-TiO_2/EP can be obtained. These S-TiO_2/EP pre-polymer matrixes were then poured into a pre-heated mould under 80 ℃, and degassed at 80 °C for about 30 min in a vacuum drying oven, until the bubbles inside the matrix are completely removed. Finally, the moulds filled with S-TiO_2/EP pre-polymer were put into the blast drying oven, and cured with the cured process of 80 °C/1 h + 100 °C/1 h + 120 °C/2 h.

2.4 Measurements

2.4.1 The X-ray Diffraction (XRD)

The X-ray diffraction (XRD, Bruker D8, Germany) was employed to research the crystal structure of S-TiO_2 at room temperature.

2.4.2 Scanning Electron Microscopy (SEM)

The S-3400N II scanning electron microscope (SEM, HITACHI, Japan) was employed to observe the morphology of S-TiO_2, and the surface morphology of the fractured surface of the EP and S-TiO_2/EP samples at room temperature.

2.4.3 Dielectric Properties

The dielectric properties of EP and S-TiO_2/EP composites were measured by dielectric constant dielectric loss tester (ZJD-A type, China Aviation Times Company).

2.4.4 Thermal Conductivity

The thermal conductivities of the EP and S-TiO_2/EP composites were measured by transient fast hot wire method of thermal conductivity tester (KDRX-II, Xiangtan Xiangyi Instrument Co., Ltd, China).

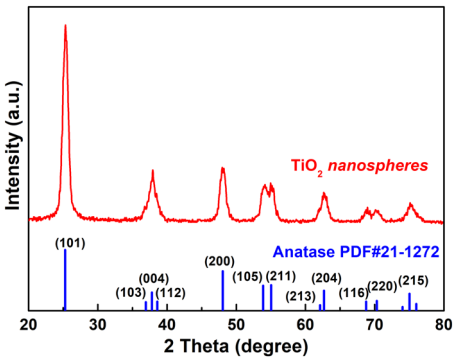

Fig. 3 The XRD result of S-TiO_2

3 Results and Discussion

3.1 Morphology Structure of the S-MoS_2

The crystallographic structure of S-TiO_2 is researched by X-ray diffraction (XRD) as shown in Fig. 3. As can be seen from the figure, the strong diffraction peaks appear at $2\theta = 25.25°$, 37.83°, 48.03°, 53.91°, 55.01°, 62.61°, 68.94°, 70.35°, 75.04° can be correspond to standard spectrum (21-1272) of anatase TiO_2 which is (101), (004), (200), (105), (211), (204), (116), (220) and (215), respectively. At the same time, there is no excess impurity peak on the way, indicating that the prepared S-TiO_2 possesses good crystal shape and high purity. In addition, the diffraction peak corresponding to S-TiO_2 is weak and wide, which is caused by the small grain size of the nanoparticles.

To research the morphology of the obtained S-TiO_2 particles, The SEM with different magnification ratios is employed to observe their apparent morphology. It can be seen from Fig. 4A, the surface of the obtained S-TiO_2 particles is more loose and uniform, and the pore size is smaller, indicating that the prepared S-TiO_2 are ultrafine powders, which is benefit to alter their aggregation state in the resin system. In order to further observe the microscopic morphology of S-TiO_2 particles, the SEM of the part marked in red in Fig. 4A was magnified by 25 times, and the results were shown in Fig. 4B. It can be seen that S-TiO_2 nanoparticles are spherical morphology with uniform particle size, which can endow the S-TiO_2 with excellent stability.

3.2 Dielectric Properties of the Materials

The dielectric constant of S-TiO_2/EP composites with different S-TiO_2 content was measured with frequency, and the corresponding curve was as shown in Fig. 5. It can be observed from the figure that the dielectric constant of

Fig. 4 The SEM of S-TiO_2

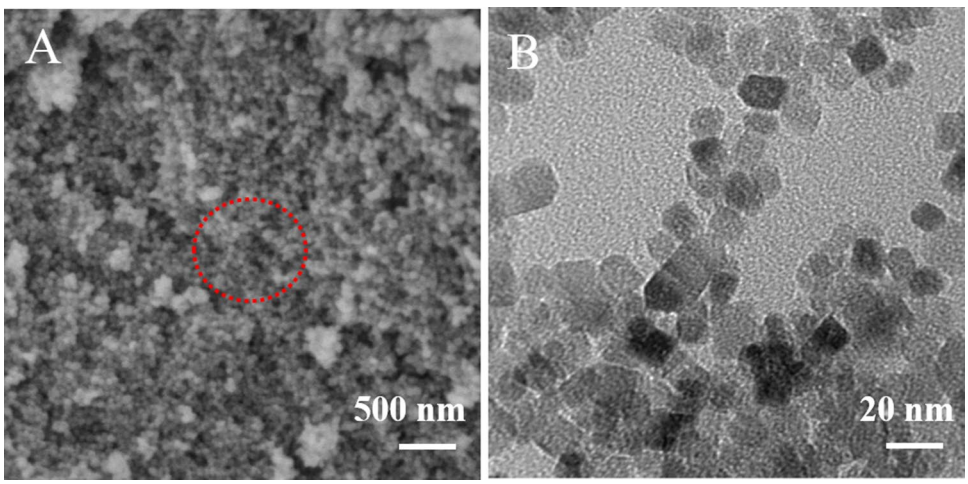

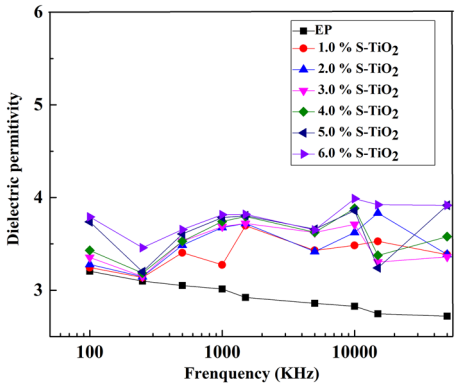

Fig. 5 The dielectric permittivity of S-TiO_2/EP with different content of S-TiO_2 varies by frequency

S-TiO_2/EP composites increases with the increase of S-TiO_2 content, but the increase amplitude is not high, indicating that even the addition of S-TiO_2 can increase the dielectric constant of S-TiO_2/EP composites to a certain extent, but it is still within the range of use. At the same time, the dielectric constant did not increase or decrease significantly with the increase of frequency, and the dielectric constant was still low above 1000 kHz, indicating that even with the addition of a certain amount of S-TiO_2, the S-TiO_2/EP composites were still difficult to turn polarization at high frequency, so it had a low dielectric constant drop. The low dielectric constant of S-TiO_2/EP composites at high frequencies can greatly meet the needs of their use as high frequency insulating electronic materials.

Figure 6 shows the curve of dielectric loss of EP and S-TiO_2/EP composites with different S-TiO_2 content as a function of frequency. As can be observed from the figure, when S-TiO_2 content was lower than 4.0 wt%, the dielectric loss of S-TiO_2/EP composite was close to that of pure EP, and even showed a lower trend at a certain frequency. However, as the S-TiO_2 content continues to further increase, the dielectric loss of S-TiO_2/EP composites began to increase, this is because of excessive S-TiO_2 inside the composites prone to stack, and caused a local interfacial area overlap, which provides a good path for carriers to form the current conduction, thereby the dielectric loss of S-TiO_2/EP composite became to increase. In addition, it also can be observed from the figure, with the increase of frequency, the dielectric loss of EP and S-TiO_2/EP composites also began to increase, this phenomenon is mainly due to the increase of the frequency can cause the acceleration of internal polarity molecular motion, and the heat generated by the friction between the molecular chain also increased, which resulted in the increase of dielectric loss by the composite. However, the presence of S-TiO_2 that inhibit the movement of carriers to a certain extent, while the dielectric loss of S-TiO_2/EP composites does not increase too much, thus it can meet the requirements of its use as a high frequency circuit.

3.3 Thermal Conductivities of the Materials

The effect of S-TiO_2 doges on the thermal conductivities of S-TiO_2/EP composites are also researched, and the results are shown in Fig. 7. As can be seen from the figure that the thermal conductivities of S-TiO_2/EP composites increase by the increase of S-TiO_2 content, and reached the maximum value of 0.1976 W/mK when the content of S-TiO_2 is 4.0 wt%, increased as much as 16.2% compared with pure EP resin, suggesting that the properly addition of S-TiO_2 can obviously improve the thermal conductivities of EP. The enhanced thermal conductivity of S-TiO_2/EP composites can be attributed to the essential excellent thermal conductivity of S-TiO_2. To further research the reasons for the improvement of thermal conductivity of the materials, the fracture surface morphology of EP resin and S-TiO_2/EP composites filled with 4.0 wt% S-TiO_2 are observed by SEM. As can be seen from the figure, the surface of pure EP resin is very flat, while the surface of the S-TiO_2/EP composite can be observed with regular bumps, which is caused by the

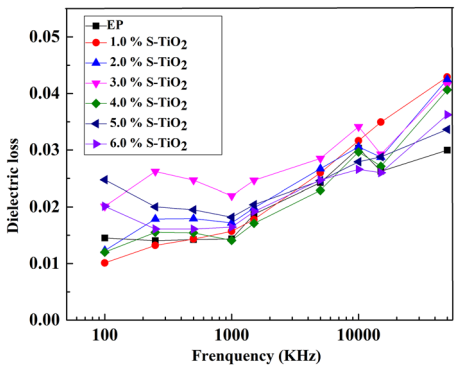

Fig. 6 The dielectric loss of S-TiO_2/EP with different content of S-TiO_2 varies with frequency

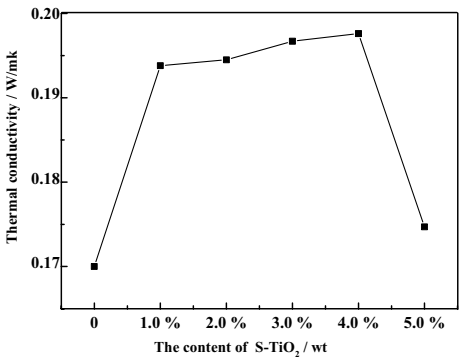

Fig. 7 The thermal conductivities of S-TiO_2/EP with different content of S-TiO_2

uniform dispersion of S-TiO_2 inside the resin. The uniform dispersion of S-TiO_2 can provide a good thermal conduction path for heat conduction inside the resin, which is conducive to the improvement of thermal conductivity of the material. However, when the content of S-TiO_2 further increased to 5.0 wt%, the thermal conductivity of the S-TiO_2/EP composites began to decrease significantly. This phenomenon is due to the presence of a small amount of hydroxyl groups on the surface of the S-TiO_2 prepared by the method of hydrating heat. Therefore, excessive S-TiO_2 is unevenly dispersed in the EP matrix, resulting in some voids. The defects caused by such voids will hinder the heat transfer and ultimately lead to the decrease of the thermal conductivity of the S-TiO_2/EP composites (schematic diagram of heat conduction mechanism is shown in Fig. 9). Even as so, S-TiO_2/EP composites with high content of S-TiO_2 still exhibit better thermal conductivity than that of pure EP resin.

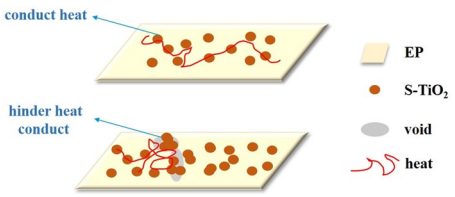

Fig. 9 Schematic diagram of heat conduction mechanism

3.4 Mechanical Properties of the Materials

When used as electronic and electrical materials, the mechanical property of EP composites is also very important. Figure 10 shows the influence of different contents of S-TiO_2 on the flexural strength of S-TiO_2/EP composites. It can be seen from the figure that the flexural strength of S-TiO_2/EP composites increases firstly and then decreases slightly with the further increase of S-TiO_2 content. When S-TiO_2 content increased to 4.0 wt%, the flexural strength of S-TiO_2/EP composite reached the maximum of 96.18 MPa, which was increased by 29.4% compared with that of pure EP resin (74.32 MPa). This indicates that the reasonable addition of S-TiO_2 can effectively improve the mechanical properties of EP resin. It is because when the reasonable addition of S-TiO_2 is added into EP resin, the ultrafine S-TiO_2 is conducive to the uniform dispersion in the resin matrix, and the spherical structure of S-TiO_2 can be deformed under the action of external forces, effectively resisting the damage of external forces on the composites. However, when further increasing the S-TiO_2 content, the flexural strength of S-TiO_2/EP composite no longer increases, even started to decline slightly, the reason for this is that too much S-TiO_2 in the composites start to serious reunion, caused the internal defects of S-TiO_2/EP composite, which seriously affect their mechanical properties.

It can also be observed from the SEM result as shown in Fig. 8A that, the fracture morphology of pure EP resin has a very smooth cross section and smooth structure, showing an obvious river-like morphology, which is a typical brittle fracture characteristic, indicating that pure EP resin exhibits limited mechanical properties. However, when the appropriate content of S-TiO_2 (4.0 wt%) was added, the fracture surface of S-TiO_2/EP composite (as shown in Fig. 8B) became very rough and appeared obvious fish scale shape. At the same time, more dense dimples were observed than pure EP, showing typical ductile fracture characteristics, indicating that the mechanical properties of the S-TiO_2/EP composites increased after the addition of S-TiO_2. At the same time, it can also be observed from Fig. 8B that there are a small number of obvious protrusions on the fracture surface and the distribution is relatively uniform. Such protrusions are attributed to the S-TiO_2 particles, which indicates that S-TiO_2 has achieved good dispersion in the EP composites.

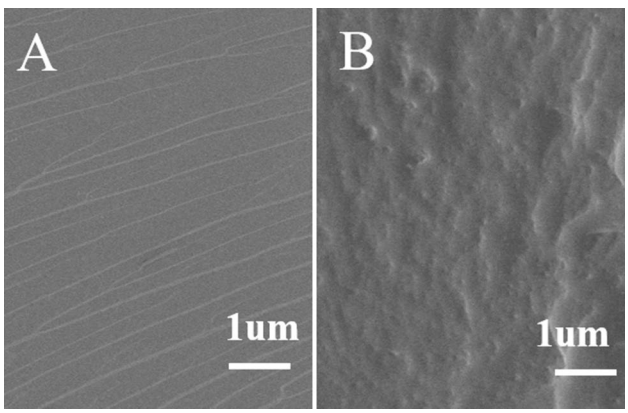

Fig. 8 SEM of fracture surfaces taken from the resins (**A** EP, **B** S-TiO_2/EP composites with 4.0 wt% S-TiO_2)

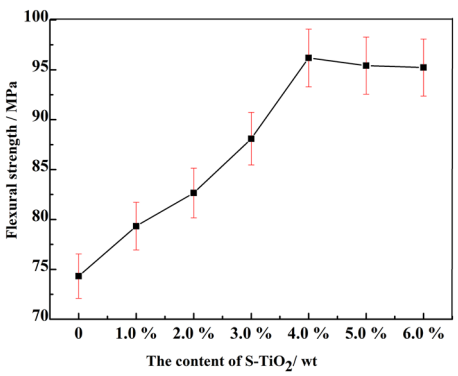

Fig. 10 The flexural strength of the S-TiO_2/EP composites with different content S-TiO_2

4 Conclusions

A novel S-TiO_2 dioxide superfine powders with microspheres structure (S-TiO_2) were prepared via hydrothermal process, and the S-TiO_2 was then employed as modifiers to prepare S-TiO_2/EP composites by blending with EP matrix. The results suggested that dielectric constant of S-TiO_2/EP composites was improved and their dielectric loss can still remain a low level even under high frequency. Furthermore, the reasonable addition of S-TiO_2 can also enhance the thermal conductivity of S-TiO_2/EP, thermal conductivities of S-TiO2/EP composites reached the maximum value of 0.1976 W/mK when the content of S-TiO_2 is 4.0 wt%, increased as much as 16.2% compared with pure EP resin, which is owning to the good thermal conductivity of S-TiO_2 itself and the thermal conductivity path formed by S-TiO_2 inside the EP matrix. However, excessive addition of S-TiO_2 is detrimental to the thermal conductivity of S-TiO_2/EP composites, which is attributed to the voids inside the materials caused by the agglomeration of S-TiO_2. Meanwhile, the flexural strength of S-TiO_2/EP composite with 4.0 wt% S-TiO_2 also reached the maximum of 96.18 MPa, increased by 29.4% compared to pure EP resin (74.32 MPa). The purpose of this study is to prepare a kind of resin composites with good thermal conductivity and excellent dielectric properties which can be used in high frequency electric field.

Acknowledgements This work was financially supported by the Natural Science Research Program of Shaanxi Province (2021JQ-798), the Scientific Research Program of Education Department of Shaanxi Province (21JK0870), Xi 'an Association for Science and Technology Young Talent Promotion Project (095920211335), the Environmental Pollution Monitoring and Control Innovation Team of Education Department of Shaanxi Province (51), and the Research Team of Xi'an University (XAWLKYTD018).

References

1. R. Dou, C. Shen, B. Yin et al., Tailoring the impact behavior of polyamide 6 ternary blends via a hierarchical coreshell structure in situ formed in melt mixing. RSC Adv. **5**, 14592–14602 (2015)
2. Y. Liu, J.M. Chen, Y.X. Qi et al., Cross-linked liquid crystalline polybenzoxazines bearing cholesterol-based mesogen side groups. Sci. Direct Polym. **145**, 252–260 (2018)
3. M. Liu, W. Jiang, Q. Chen et al., A facile one-step method to synthesize SiO_2@polydopamine core-shell nanospheres for shear thickening fluid. RSC Adv. **6**(35), 29279–29287 (2016)
4. S. Cui, X. Kang, W. Cai, S. Zhang, Revealing the formation mechanism of insoluble polydopamine by a simplified model system. Polym. Chem. **8**, 860–864 (2017)
5. L. Yang Wang, J. Zhu, Zhou et al., Dielectric properties and thermal conductivity of epoxy resin composite modified by Zn/ZnO/Al_2O_3 core-shell particles. Polym. Bull. **76**, 3957–3970 (2019)
6. O. Eksik, S.F. Bartolucci, T. Gupta et al., A novel approach to enhance the thermal conductivity of epoxy nanocomposites using graphene core-shell additives. Carbon **101**, 239–244 (2016)
7. T. Chen, X. Chen, M. Wang et al., A novel halogen-free co-curing agent with linear multi-aromatic rigid structure as flame-retardant modifier in epoxy resin. Polym. Adv. Technol. **29**, 1–9 (2017)
8. Q. Yong, V. Wachtendorf, P. Klack et al., Improved flame retardancy by synergy between cyclotetrasiloxane and phosphaphenanthrene/triazine compounds in epoxy thermoset Polym. Int. **66**, 1883–1890 (2017)
9. H. Sensen, M. Qingshi, A. Sherif et al., Mechanical and electrical properties of graphene and carbon nanotube reinforced epoxy adhesives: experimental and numerical analysis. Compos. A **120**, 116–126 (2019)
10. J. Wenqi Yu, P. Fu, Chen et al., Enhanced thermal conductive property of epoxy composites by low mass fraction of organic-inorganic multilayer covalently grafted carbon nanotubes. Compos. Sci. Technol. **125**, 90–99 (2016)
11. X. Xu, S. Gao, D. Zhang et al., Mechanical behavior of liquid nitrile rubber -modified epoxy resin: experiments, constitutive model and application. Int. J. Mech. Sci. **151**, 46–60 (2019)
12. Y. Xinran Shan, Z. Liu, Wu et al., Preparation and property study of graphene oxide reinforced epoxy resin insulation nanocomposites with high heat conductivity. Mater. Sci. Eng. **171**, 012151 (2017)
13. A.M. Islam, H. Lim, N.H. You et al., Enhanced thermal conductivity of liquid crystalline epoxy resin using controlled linear polymerization. ACS Macro Lett. **7**, 1180–1185 (2018)
14. H. Guo, J. Zheng, J. Gan et al., High thermal conductivity epoxies containing substituted biphenyl mesogenic. J. Materi. Sci.: Mater. Electron. **27**, 2754–2759 (2016)
15. C. Yu Wang, Q. Yang, Pei et al., Some aspects on thermal transport across the interface between graphene and epoxy in nanocomposites. ACS Appl. Materi. Interfaces **8**, 8272–8279 (2016)
16. W. Yuan, Q. Xiao, L. Li et al., Thermal conductivity of epoxy adhesive enhanced by hybrid grapheneoxide/AlN particles. Appl. Therm. Eng. **106**, 1067–1074 (2016)
17. Hu. Yong, G. Du, N. Chen et al., A novel approach for Al_2O_3/epoxy composites with high strength and thermal conductivity. Compos. Sci. Technol. **124**, 36–43 (2016)
18. H. Helezi Zhou, X. Wang, Du et al., Facile fabrication of large 3D graphene filler modified epoxy composites with improved thermal conduction and tribological performance. Carbon (2018). https://doi.org/10.1016/j.carbon.2018.07.059
19. W. Chen, Z. Wang, C. Zhi, High thermal conductivity and temperature probing of copper nanowire/upconversion nanoparticles/epoxy composite. Compos. Sci. Technol. **130**, 63–69 (2016)
20. W.S. Zhi, J. Kibsgaard, C.F. Dickens et al., Combining theory and experiment in electrocatalysis: insights into materials design Science **355**(6321), 1–12 (2017)
21. P. Nasehi et al., Preparation and characterization of a novel Mn-Fe2O4 nanoparticle loaded on activated carbon adsorbent for kinetic, thermodynamic and isotherm surveys of aluminum ion adsorption. Sep. Sci. Technol. **55**(6), 1078–1088 (2020)
22. P. Nasehi, S.F. Abbaspour, R. Asadi, Cr (VI) adsorption using synthesis novel UIO-66-$MnFe_2O_4$-TiO_2 magnetic nanoparticles by experimental design. J. Appl. Res. Chem.-Polym. Eng. **4**(4), 33–48 (2021)
23. B.B. Adormaa, W.K. Darkwah, Y. Ao, Oxygen vacancies of the TiO2 nano-based composite photocatalysts in visible light responsive photocatalysis. RSC Adv. **8**(58), 33551–33563 (2018)

24. J. Towfighi, Vanadium oxide supported on Al-modified titania nanotubes for oxidative dehydrogenation of propane. J. Chem. Pet. Eng. **51**(2), 113–121 (2017)
25. Boshra, Mahmoudi, Seyed Foad Abbaspour, and Mojtaba Saei Moghaddam. Cadmium adsorption using novel $MnFe_2O_4$-TiO_2-UIO-66 magnetic nanoparticles and condition optimization using a response surface methodology. RSC Adv. **9**(35), 20087–20099 (2019)
26. J. Sung, M. Shin, P.R. Deshmukh et al., Preparation of ultrathin TiO_2 coating on boron particles by thermal chemical vapor deposition and their oxidation-resistance performance. J. Alloys Compd. **767**, 924–931 (2018)